

Theory of cyclotron resonance for electrons in a Si surface inversion layer under a uniaxial stress

C. S. Ting

Department of Physics, University of Houston, Houston, Texas 77004

A. K. Ganguly

Naval Research Laboratory, Washington, D. C. 20375

W. Y. Lai

Department of Physics, University of Houston, Houston, Texas 77004

(Received 19 March 1981)

The theory of cyclotron resonance for two types of carriers under a uniaxial stress is studied by using the method of kinetic equations. The intervalley electron-electron relaxation rate $\tau_e^{-1}(\omega)$ is obtained by using the memory-function approach at finite temperatures. The contributions from both the imaginary and real parts of $\tau_e^{-1}(\omega)$ to the cyclotron-resonance line shape are considered. The cyclotron-resonance mass as a function of temperature has been obtained. The agreement between our results and experimental measurements seems to be satisfactory.

I. INTRODUCTION

On the Si(100) surface of a metal-oxide—semiconductor structure there are two sets of non-equivalent subbands¹—one with two degenerate valleys at the center of the two-dimensional Brillouin zone and the other with four degenerate valleys centered near the corners along $\langle 100 \rangle$ directions. The subbands of the center valleys are energetically lower than those of the corner valleys. At zero temperature and not too high electron density, only the center valleys are occupied. In the presence of a magnetic field H , the center of mass of the electrons performs cyclotron motion with a single cyclotron frequency given by $\omega_1 = -eH/m_1c$, where $m_1 \simeq 0.195m_e$ is the bare effective mass for electrons in the center valleys, m_e and e are the mass and charge of a free electron, respectively and c is the speed of light. As the temperature is raised, thermal occupation of the subbands associated with the corner valleys by electrons begins to take place. In a cyclotron-resonance experiment an additional resonance peak should occur at $\omega_2 \simeq eH/m_2c$ ($m_2 \simeq 0.4m_e$). the application of a uniaxial stress is expected to have the same effect as raising the temperature. Compression along a $\langle 100 \rangle$ direction causes two of the four corner valleys to be lowered in energy with respect to the center valleys.² At suitable carrier densities there should be partial oc-

cupation of both these subbands and two distinct resonances are expected. Earlier experiments at low electron concentration ($n \simeq 0.5 \times 10^{12} \text{ cm}^{-2}$) showed that the cyclotron-resonance spectrum could be fitted satisfactorily with a single-resonance line shape.^{3,4} A theory of Kelley and Falicov⁵ who proposed the existence of charge-density wave states on the silicon (100) surface by assuming an extremely large intervalley electron-electron coupling, predicted a single resonance at zero temperature.

The effect of intervalley Coulomb scattering on the cyclotron line shape was studied by Appel and Overhauser⁶ using the equation of motion method, and also by Takada and Ando⁷ using the Fermi-liquid theory. both of these approaches^{6,7} are valid in the limits of $T \ll E_F^{(i)}$ and $\omega \ll E_F^{(i)}$. Here ω is the frequency of the applied ac electric field. $E_F^{(i)}$ ($i = 1,2$) is the Fermi energy of the carriers in either the center or the corner valleys. One of the essential features of these results^{6,7} is that there are always two resonance peaks at low temperature if the impurity effect on the single-particle relaxation time is not too strong. A recent experiment⁸ on the cyclotron resonance under uniaxial stress indeed shows two resonance peaks at carrier density $n \simeq 1.2 \times 10^{12} \text{ cm}^{-2}$. For the present paper we wish to study this problem by using the method of Appel and Overhauser.⁶ The primary differences between our method and that of Ref. 6 are as fol-

lows. (a) The intervalley scattering rate $\tau_e^{-1}(\omega)$ will be calculated to higher temperature using the memory-function approach. (b) The effect due to the imaginary part of $\tau_e^{-1}(\omega)$ will be considered. (c) The single-particle relaxation times τ_1 and τ_2 for electrons in the center and corner valleys, respectively, will be calculated from the first principle by the method described in Ref. 9 using the impurity concentration as the only input parameter. In Ref. 6 the values of τ_1 and τ_2 are arbitrarily chosen and the effect due to the imaginary part of $\tau_e^{-1}(\omega)$ is neglected. As we shall see later, the imaginary part of $\tau_e^{-1}(\omega)$ shifts the cyclotron mass of the carriers. In Sec. II, we shall briefly describe the method of equation of motion and give the expression for the conductivity of two types of carriers. In Sec. III the connection between the intervalley electron-electron relaxation rate $\tau_e^{-1}(\omega)$ and the memory function will be given. The real part and the imaginary part of $\tau_e^{-1}(\omega)$ shall be calculated using the random-phase and the plasmon-pole approximations, respectively. In Sec. IV the numerical result of our calculation will be presented. We shall show that with a fixed impurity (oxide charge) concentration, there is only one resonance peak in the resonance spectrum for the carrier density $n = 0.5 \times 10^{12} \text{ cm}^{-2}$. However, when the carrier density is increased to $n = 1.2 \times 10^{12} \text{ cm}^{-2}$ there are two resonance peaks. This feature is in agreement with experiments.^{4,8} The resonance spectra as a function of the applied magnetic field at different temperatures and under several uniaxial stresses will be given. We also present the results for the resonance mass as a function of temperature at $n = 1.2 \times 10^{12} \text{ cm}^{-2}$ for different uniaxial stresses. The final section contains a discussion of the present results and its connection with previous works.^{6,7}

II. THE ac CONDUCTIVITY OF A TWO-COMPONENT PLASMA IN THE PRESENCE OF A MAGNETIC FIELD

The magnetoconductivity for a system consisting of two types of carriers has been studied previously.⁶ We shall briefly describe this method and present the final results. Our system is made of n_1 carriers with charge e_1 and mass m_1 from the center valleys (type-1), and n_2 carriers with charge e_2 and mass m_2 from the corner valleys (type-2). Let \vec{P}_1 and \vec{P}_2 be the total momenta of electrons of type-1 and type-2 and in the presence of both an ac electric field $\vec{E} = \vec{E}_0 e^{-i\omega t}$ and a static magnetic field H , they satisfy the following equations¹⁰:

$$-i \left[\omega + \frac{i}{\tau_1} \right] \vec{P}_1 = e_1 n_1 \left[\vec{E} + \frac{1}{cn_1 m_1} \vec{P}_1 \times \vec{H} \right] - \frac{\vec{P}_R}{\tau_e(\omega)}, \quad (1)$$

$$-i \left[\omega + \frac{i}{\tau_2} \right] \vec{P}_2 = e_2 n_2 \left[\vec{E} + \frac{1}{cn_2 m_2} \vec{P}_2 \times \vec{H} \right] + \frac{\vec{P}_R}{\tau_e(\omega)}, \quad (2)$$

where c is the speed of light, τ_i is the single-particle-transport lifetime due to scatterings with impurities, surface roughness, and phonons for carriers of type i , $\tau_e(\omega)$ corresponds to the relaxation "time" between these two types of carriers. \vec{P}_R is the relative momentum between carriers 1 and 2, with the following expression:

$$\vec{P}_R = \mu \left[\frac{\vec{P}_1}{n_1 m_1} - \frac{\vec{P}_2}{n_2 m_2} \right], \quad (3)$$

where $\mu = n_1 m_1 n_2 m_2 / (n_1 m_1 + n_2 m_2)$. If we regard the total masses of carriers 1 and 2 as, respectively, $n_1 m_1$ and $n_2 m_2$, then μ is the "total" reduced mass.

Now let us assume that the electric field is parallel to the oxide-semiconductor interface (the x - y plane) and the magnetic field H is directed along the z axis. It is straightforward to show that the x component of the current is given by $J_x = \sigma_{xx} E_{xx} + \sigma_{xy} E_y$. The conductivity tensors σ_{xx} and σ_{xy} can be obtained by solving Eqs. (1) and (2). In the present work we need the electrical conductivity for a circular polarized electric field, namely $\sigma_+ = \sigma_{xx} + i\sigma_{xy}$. After lengthy algebra, we obtain

$$\sigma_+(\omega) = \frac{iY}{\Delta} \left[\frac{e_1^2 n_1}{m_1} W_2^{(-)} + \frac{e_2^2 n_2}{m_2} W_1^{(-)} + e_1 e_2 \left[\frac{n_1 a}{m_2} + \frac{n_2 b}{m_1} \right] \right], \quad (4)$$

with

$$W_1^{(\pm)} = \omega_1 \pm \omega_{c1} + a,$$

$$W_2^{(\pm)} = \omega_2 \pm \omega_{c2} + b,$$

$$Y = W_1^{(+)} W_2^{(+)} - ab,$$

$$\Delta = [(\omega_1 + a)(\omega_2 + b) - ab]^2 + (\omega_{c1} \omega_{c2} - ab)^2 - \omega_{c1}^2 (\omega_2 + b)^2 - \omega_{c2}^2 (\omega_1 - a)^2 - a^2 b^2,$$

$$\omega_j = \omega + i/\tau_j,$$

$$\omega_{cj} = \frac{-e_j H}{m_j c} \quad (j = 1, 2),$$

$$a = \frac{i\mu}{n_1 m_1 \tau_e(\omega)},$$

and

$$b = \frac{i\mu}{n_2 m_2 \tau_e(\omega)}.$$

For later reference, we expand $\sigma_+(\omega)$ in the above equation to first-order terms in the electron-electron relaxation $1/\tau_e(\omega)$

$$\begin{aligned} \sigma_+(\omega) \simeq & \frac{ie_1^2 n_1}{m_1(\omega_1 - \omega_{c1})} + \frac{ie_2^2 n_2}{m_2(\omega_2 - \omega_{c2})} \\ & + \left[\frac{e_1}{m_1(\omega_1 - \omega_{c1})} - \frac{e_2}{m_2(\omega_2 - \omega_{c2})} \right]^2 \\ & \times \frac{\mu}{\tau_e(\omega)}. \end{aligned} \quad (5)$$

The expression for the electron-electron relaxation time $\tau_e(\omega)$ in terms of the density-density correlation functions will be given in the next section.

III. EXPRESSION FOR THE RELAXATION TIME $\tau_e(\omega)$

The derivation of the intervalley electron-electron relaxation time $\tau_e(\omega)$ in terms of the memory function¹¹ was given previously,^{12,13} and the procedure will not be repeated here. If $\tau_e^{-1}(\omega)$ is evaluated only to the lowest order in the intervalley electron-electron interaction $V_{12}(q)$, we have $\tau_e^{-1}(\omega) = -iM(\omega)$ and the memory function $M(\omega)$ is given by¹³

$$\begin{aligned} M(\omega) = & -\frac{1}{\mu\omega} \sum q_x^2 |V_{12}(q)|^2 \\ & \times [S_R(q, \omega) - S_R(q, 0)]. \end{aligned} \quad (6)$$

$S_R(q, \omega)$ here is the four-particle-correlation function

$$\begin{aligned} S_R(q, \omega) = & -i \int_{-\infty}^{\infty} dt e^{i\omega t} \Theta(t) \\ & \times \langle [D(\vec{q}, t), D(-\vec{q}, 0)] \rangle, \end{aligned} \quad (7)$$

$$D(\vec{q}, t) = \rho_{\vec{q}}^{(1)}(t) \rho_{-\vec{q}}^{(2)}(t), \quad (8)$$

where $\rho_{\vec{q}}^{(k)} = \sum_j e^{i\vec{q} \cdot \vec{r}_j} k_j$ is the density operator for type k ($k = 1, 2$) electrons. It has been pointed out

previously¹⁴ that the ordinary inverse relaxation time corresponds to the real part of $\tau_e^{-1}(\omega)$ or the imaginary part of the memory function $M(\omega)$. One of the functions of the imaginary part of $\tau_e^{-1}(\omega)$, as can be seen from Eqs. (2) and (3), is to shift the resonance frequencies or the effective masses m_1 and m_2 associated with the center and corner valleys. The effect of this term on the cyclotron-resonance spectrum has not been investigated in Ref. 6. One of the purposes of the present work is to study its influence. It is possible to compute the four-particle-correlation function $S_R(q, \omega)$ in the presence of a magnetic field by the method described in Ref. 15. However, the resonance spectrum depends critically on the lifetime broadenings of the Landau levels. There seems no unique way to obtain the values for these broadenings. In order to decrease the parameters involved with the present problem, we shall evaluate $M(\omega)$ in the absence of a magnetic field. The finite-temperature Green's function $S(q, i\omega)$ appearing in Eq. (8) can be shown to have the form

$$S(\vec{q}, i\omega) = T \sum_{n=-\infty}^{\infty} X^{(1)}(\vec{q}, i\omega - i\omega_n) X^{(2)}(-\vec{q}, i\omega_n). \quad (9)$$

The correlation function $S_R(\vec{q}, \omega)$ is obtained from the relation $S(\vec{q}, \omega + i\delta) = S_R(\vec{q}, \omega)$. In the above equation $\omega_n = 2\pi nT$. $X^{(k)}(\vec{q}, \omega + i\delta) = X_R^{(k)}(q, \omega)$ is the density-density correlation function for electron of type k ($k = 1, 2$). In general, the Green's function $X(\vec{q}, \omega)$ in random-phase approximation can be written as

$$X(\vec{q}, \omega) = \frac{\pi(\vec{q}, \omega)}{1 - V(q)\pi(\vec{q}, \omega)}, \quad (10)$$

where $V(q)$ is the intravalley electron-electron interaction. $\pi_R(\vec{q}, \omega)$ is the density-density correlation function for noninteracting electrons. It has the following expression.

$$\pi_R(\vec{q}, \omega) = 2n_v \sum_{\vec{k}} \frac{n(\vec{k}) - n(\vec{k} + \vec{q})}{\omega - \epsilon(\vec{k} + \vec{q}) + \epsilon(\vec{k}) + i\delta}, \quad (11)$$

where n_v is the valley degeneracy and $n(k)$ is the Fermi function $\epsilon(k) = k^2/2m$.

If we write $\pi_R(\vec{q}, \omega) = -(2/\pi)mF(\vec{q}, \omega)$, the function $F(\vec{q}, \omega)$ can be reduced to a single integration. Its real and imaginary parts are given by⁹

$$\text{Re}F(q, \omega) = \frac{n_v}{8\eta} \int_0^1 \frac{d\xi}{\sqrt{1-\xi}} \times \left[\frac{B}{e^{(B^2\xi/4\eta-u)\xi_0} + 1} - \frac{A}{e^{(A^2\xi/4\eta-u)\xi_0} + 1} \right], \quad (12)$$

$$\text{Im}F(q, \omega) = \frac{n_v}{4\sqrt{\eta\xi_0}} \int_0^1 \frac{d\xi}{\sqrt{-\ln\xi}} \times \left[\frac{1}{e^{(A^2/4\eta-u)\xi_0} + \xi} - \frac{1}{e^{(B^2/4\eta-u)\xi_0} + \xi} \right]. \quad (13)$$

Here we have set the Boltzmann constant $k_B = 1$, $\eta = q^2/2mE_0$, $\alpha = \omega/E_0$, $A = \alpha - \eta$, $B = \alpha + \eta$, $\xi_0 = E_0/T$, and $u = E_F(T)/E_0$, with $E_F(T)$ the Fermi energy and E_0 a suitable constant with energy units. It is straightforward to show that Eqs. (12) and (13) are independent of E_0 . The correlation function $X^{(i)}(q, \omega)$ appearing in Eq. (9) can be obtained from Eq. (10) by replacing $V(q)$, m , n_v , and E_F by $V_{ii}(q)$, m_i , $n_v^{(i)}$, and $E_F^{(i)}$, respectively. The Fermi energies $E_F^{(1)}$ and $E_F^{(2)}$ satisfy the equation of charge conservation $n = n_1 + n_2$:

$$n_i = \frac{n_v^{(i)} m_i T}{\pi} \ln(1 + e^{u_i}), \quad (14)$$

where $u_i = E_F^{(i)}/T$. $E_F^{(1)}$ and $E_F^{(2)}$ are also connected by the relation $E_F^{(1)} = E_F^{(2)} + \Delta$. Δ is the energy difference between the lowest sublevels of the corner valley and the center valley. The frequency summation in Eq. (9) can be carried out by the standard method.¹⁶ We have

$$\text{Re}S_R(\vec{q}, \omega) = \int_0^\infty \frac{d\omega'}{2\pi} \coth\left[\frac{\omega'}{2T}\right] [\text{Im}X_R^{(1)}(\vec{q}, \omega')\phi^{(2)}(-\vec{q}, \omega', \omega) + \text{Im}X_R^{(2)}(-\vec{q}, \omega')\phi^{(1)}(\vec{q}, \omega', \omega)], \quad (15)$$

$$\text{Im}S_R(\vec{q}, \omega) = \int_{-\infty}^\infty \frac{d\omega'}{2\pi} \left[\coth\left[\frac{\omega'}{2T}\right] - \coth\left[\frac{\omega' - \omega}{2T}\right] \right] \text{Im}X_R^{(1)}(\vec{q}, \omega') \text{Im}X_R^{(2)}(-\vec{q}, \omega - \omega'), \quad (16)$$

with

$$\phi^{(i)}(\vec{q}, \omega', \omega) = \text{Re}X_R^{(i)}(\vec{q}, \omega' - \omega) + \text{Re}X_R^{(i)}(\vec{q}, \omega' + \omega).$$

In order to obtain the density-density correlation function $X_R^{(i)}(q, \omega)$, we need to know the effective intravalley electron-electron interaction $V_{ii}(q)$ ($i = 1, 2$). It has the standard expression¹

$$V_{ii}(q) = \frac{2\pi e^2}{\epsilon_s q} I\left[\frac{q}{b_i}\right], \quad (17)$$

$$I(x) = (1+x)^{-6} \left\{ \frac{x}{8} (33 + 54x + 44x^2 + 18x^3 + 3x^4) + 2\epsilon_s [\epsilon_s + \epsilon_0 \coth(qD)]^{-1} \right\}.$$

Here D is the thickness of the oxide layer which we take as $D = 1000 \text{ \AA}$, $\epsilon_s = 11.8$ and $\epsilon_0 = 3.8$ are, respectively, the dielectric constants of the silicon and the oxide, $b_i = 3/\langle z_i \rangle$, and the thickness of the inversion layer $\langle z_i \rangle$ with respect to carriers of type i is given by

$$\langle z_i \rangle = \frac{3}{2} \left[\frac{6\pi}{\epsilon_s a_0} \alpha_i (N_{\text{dep}} + \frac{11}{32} n) \right]^{-1/3}, \quad (18)$$

where $a_0 = 0.529 \times 10^{-8} \text{ cm}$ is the Bohr radius and N_{dep} is the total negative charges per unit area in the depletion layer. The parameters α_1 and α_2 are given by $\alpha_1 = 0.98$ and $\alpha_2 = 0.195$. Although the formulas for $\langle z_i \rangle$ have not been obtained in a self-consistent way, we believe that their values should be correct within a factor of 2. In order to evaluate $M(\omega)$ from Eq. (6), the knowledge of the intravalley electron-electron interaction $V_{12}(q)$ is

essential. It can be obtained from the following formula:

$$V_{12}(q) = \int_0^\infty dz \int_0^\infty dz' |\psi_1(z)|^2 \times |\psi_2(z')|^2 V(q, z, z'), \quad (19)$$

$$V(q, z, z') = \frac{2\pi e^2}{\epsilon_s q} \left[e^{-q|z-z'|} + \frac{\epsilon_s - \epsilon_0 \coth qD}{\epsilon_s + \epsilon_0 \coth qD} \times e^{-q(z+z')} \right]$$

$\psi_1(z)$ and $\psi_2(z)$ are the wave functions of the electron associated with the lowest subbands for the center valley and the corner valley, respectively, and $\psi_i(z)$ is given by

$$\psi_i(z) = \left(\frac{1}{2} b_i^3\right)^{1/2} z e^{-b_i z/2}. \quad (20)$$

The integration over z and z' in Eq. (22) can be easily carried out. The result for $V_{12}(q)$ is

$$V_{12}(q) = \frac{2e^2}{\epsilon_s q} \frac{(b_1 b_2)^3}{(b_1 + b_2)^6} \left[Y(b_1, b_2) + Y(b_2, b_1) + \frac{\text{oth}(qD)}{\epsilon_s + \epsilon_0 \coth(qD)} (z_1 z_2)^3 \right], \quad (21)$$

where

$$Y(b_1, b_2) = \frac{b_1 + b_2}{(b_1 + q)^3} [b_2^2 + (5b_1 + 3q)b_2 + 10b_1^2 + 15b_1 q + 6q^2],$$

$$z_1 = \frac{b_1 + b_2}{b_1 + q},$$

and

$$z_2 = \frac{b_1 + b_2}{b_2 + q}.$$

It is rather difficult to obtain a convergent result¹⁴ for $\text{Re}M(\omega)$ by using Eqs. (9)–(13) because the function $\text{Re}X_R^{(i)}(q, \omega)$ in Eq. (10) is very singular near the plasmon pole. It would be very time consuming to determine this pole numerically within the random-phase approximation (RPA). In order to reduce the computation time, we calculate $\text{Im}M(\omega)$ according to the method described above but evaluate $\text{Re}M(\omega)$ by using the plasmon pole approximation.¹⁷ We believe that this approximation for $\text{Re}M(\omega)$ should yield an almost identical result to that of RPA. Since the major contribution to $\text{Im}M(\omega)$ comes from the low lying two-particle excitations of the system, it is not possible to obtain a reliable result for $\text{Im}M(\omega)$ by using the plasmon pole approximation where all the oscillator strengths of low-lying excitations are replaced by higher-energy plasmons. In the plasmon pole approximation, the functions $\text{Re}X_R^{(i)}(q, \omega)$ and $\text{Im}X_R^{(i)}(q, \omega)$ can be written, respectively, as¹⁷

$$\text{Re}X_R(q, \omega) = \frac{\omega_p^2(q)}{v(q)} \frac{1}{\omega^2 - \omega_q^2}, \quad (22)$$

$$\text{Im}X_R(q, \omega) = \frac{\omega_p^2(q)\pi}{2v(q)\omega_q} [\delta(\omega + \omega_q) - \delta(\omega - \omega_q)], \quad (23)$$

with

$$\omega_p^2(q) = \frac{v(q)nq^2}{m},$$

$$\omega_q^2 = -\omega_p^2(q) \frac{1 - v(q)\pi(q, 0)}{v(q)\pi(q, 0)},$$

$$\pi(q, 0) = -\frac{2}{\pi} m \text{Re}F(q, 0).$$

$\text{Re}F(q, 0)$ here can be obtained from Eq. (12) by setting $\omega = 0$. $X_R^{(i)}(q, \omega)$ ($i = 1, 2$) are obtained by replacing m , E_F , n , n_v , and $v(q)$ with m_i , $E_F^{(i)}$, n_i , $n_v^{(i)}$, and $v_{ii}(q)$, respectively.

IV. RESULTS

The numerical computation is performed under the following ideal situation: We assume that a suitable uniaxial stress has been applied on Si in the $\langle 100 \rangle$ direction, which lowers the ground-state subbands of two of the four degenerate corner valleys. Then the value of the energy difference Δ between the ground state subbands of these two lower corner valleys and those of the center valleys can be easily varied. For general values of Δ , the intervalley electron-electron scattering rate $1/\tau_e(\omega)$ or the memory function $M(\omega)$ can be obtained from Eqs. (6)–(13). For our numerical computation we take $m_1 = 0.195m_e$ and $m_2 = 0.4m_e$ for carriers in the

center valley and the corner valley, respectively. Here m_e is the free-electron mass. We choose $N_{\text{dep}} = 0.3 \times 10^{12} \text{ cm}^{-2}$ for the space charge in the depletion layer. The angular frequency of the external electric field $\omega = 3.5 \text{ meV}$ is chosen according to the experimental condition.^{4,8} For carrier density $n = 0.5 \times 10^{12} \text{ cm}^{-2}$ and $\Delta = 0$, the numerical results for both the real and the imaginary parts of $M(\omega)$ as a function of the temperature are shown in Fig. 1 where the dashed line corresponds to the real part of $M(\omega)$ which, as we have mentioned previously, is calculated according to the plasmon pole approximation. The solid line corresponds to the imaginary part of $M(\omega)$ which is evaluated according to the random-phase approximation. $\text{Im}M(\omega) \propto T^2$ at low temperature, in agreement with the results of Refs. 6 and 12. However, as T increases $\text{Im}M(\omega)$ deviates from T^2 and reaches a maximum at $T \sim 120 \text{ K}$. Then it decreases slowly as $1/T$ at higher temperatures.

The essential feature of the real part of $M(\omega)$ is that its value becomes negative in the temperature range from $T \sim 20$ to 80 K and has a minimum at $T \simeq 47 \text{ K}$. The function $M(\omega)$ has also been calculated for $n = 1.2 \times 10^{12} \text{ cm}^{-2}$ with $\Delta = -1.0, 0.0$, and 2.58 meV . They correspond, respectively, to $n_1/n = 0.23, 0.33$, and 0.58 at zero temperature. The results for $\text{Im}M(\omega)$ and $\text{Re}M(\omega)$ are shown in Figs. 2 and 3, respectively. From Fig. 2 it is easy to see that the temperature dependence of $\text{Im}M(\omega)$ is similar to what we have shown in Fig. 1, and its values at fixed temperature change only slightly when Δ varies from -1.0 to 2.58 meV . The real part of $M(\omega)$ for $\Delta = -1.0 \text{ meV}$ shows a

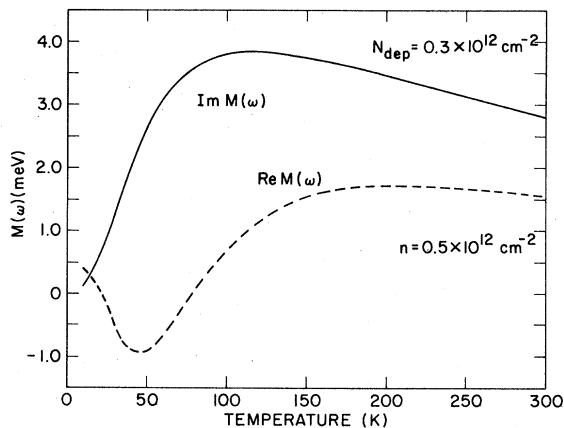


FIG. 1. The real and the imaginary parts of the memory function $M(\omega)$ are plotted as functions of temperature for $n = 0.5 \times 10^{12} \text{ cm}^{-2}$, $\Delta = 0$, and $\omega = 3.5 \text{ meV}$.

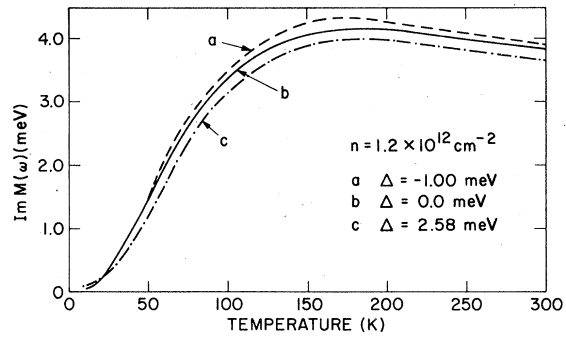


FIG. 2. The imaginary part of $M(\omega)$ is plotted as a function of T for $n = 1.2 \times 10^{12} \text{ cm}^{-2}$, $N_{\text{dep}} = 0.1 \times 10^{12} \text{ cm}^{-2}$, and three values of Δ .

minimum at $\sim 50 \text{ K}$. However, this minimum gradually disappears as the value of Δ changes from $\Delta = -1.0$ to 2.58 meV .

In order to determine the cyclotron-resonance line shape, the knowledge of the single-particle scattering rates $1/\tau_1$ and $1/\tau_2$ for the center valley and the corner valley are essential. If we attribute the single-particle scattering mechanism entirely to charged impurities, $1/\tau_1$ and $1/\tau_2$ appearing in a cyclotron-resonance experiment should correspond to the high-frequency expansion results in the memory-function approach¹⁸

$$\frac{1}{\tau_i} = \int_0^\infty \frac{E}{E_i} \left[-\frac{\partial n_i(E)}{\partial E} \right] \frac{1}{\tau_i(E)} dE, \quad (24)$$

$$\frac{1}{\tau_i(E)} = \frac{m_i n_I}{2\pi} \int_0^\infty \left| \frac{V_i(q)}{\epsilon_i(q,0)} \right| (1 - \cos\phi) d\phi,$$

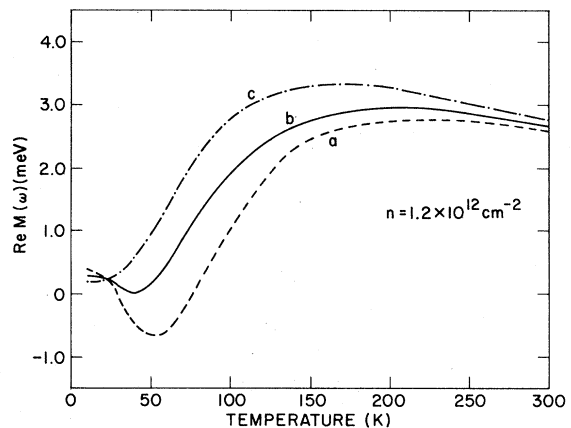


FIG. 3. The real part of $M(\omega)$ is plotted as a function of T . The parameters and notation are identical to those of Fig. 2.

where $q = 2(2m_i E)^{1/2} \sin \frac{1}{2} \phi$ and $\epsilon_i(q, 0) = 1 - V_{ii}(q)\pi_i(q, 0)$. $E_i = \pi n_i / 2m$ corresponds to the Fermi energy at $T = 0$ K for type- i electrons, n_i is the impurity concentration and $V_i(q)$, the interaction between the charged impurity and carriers of type i , is given by⁹

$$V_i = (-2\pi e^2 / \epsilon_s q) J(q/b_i),$$

with

$$J(x) = 2(1+x)^{-3} \epsilon_s (\epsilon_s + \epsilon_0 \coth Dq)^{-1}.$$

The oxide charge concentration n_I can be obtained if the mobility of the sample is known for zero external stress. In the following computation we shall take $n_I = 1.5 \times 10^{11} \text{ cm}^{-2}$ which will give the sample a mobility $\mu = 6500 \text{ cm}^2/\text{V sec}$ for $n = 7.7 \times 10^{11} \text{ cm}^{-2}$ at very low temperature. The numerical results for $1/\tau_i$ ($i = 1, 2$) as a function of temperature are shown in Fig. 4 for $n = 1.2 \times 10^{12} \text{ cm}^{-2}$. Curves 1, 2, and 3, respectively, correspond to the cases $\Delta = 2.58$, and -1.0 meV. The essential feature of the results is that at moderately low temperature $1/\tau_i$ depends linearly on T and at high temperature it decreases slowly as $1/T$. With all the necessary parameters, the real part of the conductivity $\sigma_T(\omega)$ can be computed according to Eq. (4). We have calculated the cyclotron-resonance line shape for $n = 1.2 \times 10^{12} \text{ cm}^{-2}$, $n_I = 1.5 \times 10^{11} \text{ cm}^{-2}$, and $\Delta = 0$ at temperatures $T = 10$

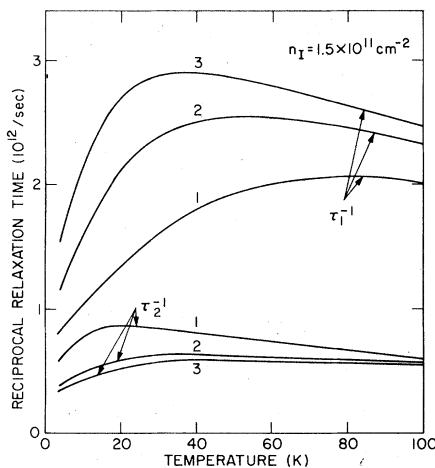


FIG. 4. The single-particle reciprocal relaxation times τ_i^{-1} ($i = 1, 2$) are plotted as a function of T for $n = 1.2 \times 10^{12} \text{ cm}^{-2}$, and $N_{\text{dep}} = 0.1 \times 10^{12} \text{ cm}^{-2}$. Curves labeled by 1, 2, and 3 correspond, respectively, to the cases $\Delta = 2.58$, 0, and -1.0 meV.

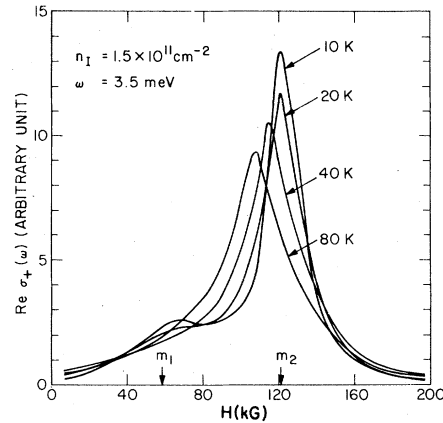


FIG. 5. The real part of the conductivity is plotted as a function of magnetic field. The impurity concentration is fixed at $n_I = 1.5 \times 10^{11} \text{ cm}^{-2}$. m_1 and m_2 indicate the positions of the resonances due to carriers with masses m_1 and m_2 , respectively, when the intervalley electron-electron interaction is neglected.

and 40 K. The results as a function of external magnetic field H are shown by solid lines in Fig. 5.

At $T = 10$ K there are two resonance peaks, while at $T = 40$ K there is only a single resonance peak. However, at lower carrier density, for example $n = 0.5 \times 10^{12} \text{ cm}^{-2}$, we obtain only a single resonance at both temperatures (dashed curves in Fig. 5). This feature seems to agree with the experimental results at low temperature in which a single resonance^{3,4} has been found for a sample with low carrier density ($n \approx 0.5 \times 10^{12} \text{ cm}^{-2}$) and at higher density ($n \approx 1.2 \times 10^{12} \text{ cm}^{-2}$) two resonance peaks appeared in the spectra.⁸ We believe that the single resonance found for $n = 0.5 \times 10^{12} \text{ cm}^{-2}$ at

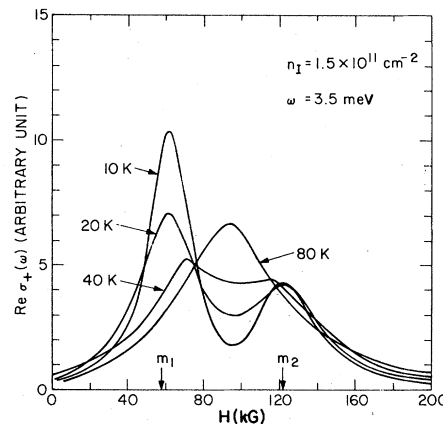


FIG. 6. The real part of the conductivity is plotted as a function of magnetic field at several different temperatures for $n = 1.2 \times 10^{12} \text{ cm}^{-2}$ and $\Delta = 2.58$ meV.

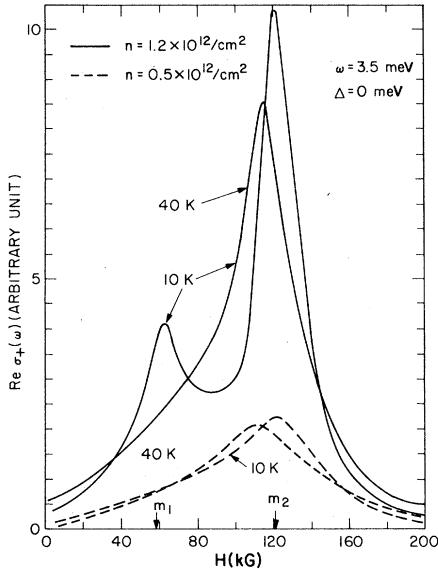


FIG. 7. The real part of the conductivity is plotted as a function of magnetic field for $n = 1.2 \times 10^{12} \text{ cm}^{-2}$ and $\Delta = -1.0 \text{ meV}$.

$T = 10 \text{ K}$ is entirely due to the fact that the single-particle scattering rate $1/\tau_1$ ($> 1/\tau_2$) becomes so large as compared to its value at $n = 1.2 \times 10^{12} \text{ cm}^{-2}$ that the resonance peak due to electrons in the center valley is completely smeared out.

The cyclotron-resonance line shapes as a function of H for the cases $\Delta = 2.58$ and -1.0 meV are presented in Figs. 6 and 7, respectively, at temperatures $T = 10, 20, 40,$ and 80 K . Our results at $T \simeq 10 \text{ K}$ agree qualitatively with the experimental measurements of Abstreiter *et al.*⁸ at low temperature, which show two resonance peaks. However, at higher temperature there is only a single peak in the resonance spectra. The cyclotron-resonance mass m^* is plotted as a function of T in Fig. 8. The dashed curve and the solid curve, respectively, represent the cases $\Delta = -1.0$ and 2.58 meV . For $\Delta = -1.0 \text{ meV}$ there are two resonance masses for $T < 40 \text{ K}$. The lower one corresponds to the renormalized electron mass of the center valley and the upper one corresponds to that of the corner valley. The values of these two masses emerge into a single value at $T = 40 \text{ K}$. At higher temperature ($T > 40 \text{ K}$) the effective mass of the resonance decreases as T increases and it finally levels off with its value slightly less than m_2 . For $\Delta = 2.58 \text{ meV}$ these two resonance peaks emerge into a single resonance for $T > 60 \text{ K}$, and the effective mass m^* derived from this single resonance peak increases slowly as T increases and $m^* \simeq 0.7m_2$ at $T \simeq 100 \text{ K}$.

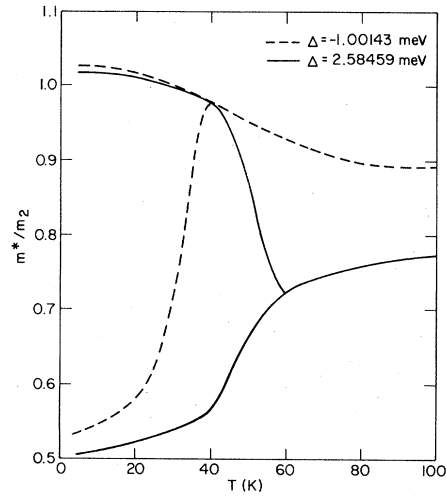


FIG. 8. The cyclotron-resonance mass m^* is plotted as a function of T for $n = 1.2 \times 10^{12} \text{ cm}^{-2}$. Here $m_2 = 0.4 m_e$, m_e being the free-electron mass.

V. DISCUSSION

In this paper we have studied the influence of the intervalley electron-electron interaction on the cyclotron-resonance line shape for electrons in the Si(100) surface inversion layers under several uniaxial stresses at finite temperatures. It can be regarded as an extension of the work by Appel and Overhauser⁶ in which the intervalley electron-electron relaxation rate $\text{Re}[1/\tau_e(\omega)]$ is evaluated only at low temperature or $T \ll E_F^{(i)}$ ($i = 1, 2$) and the influence due to $\text{Im}[1/\tau_e(\omega)]$ is neglected. In the present work we consider the contributions from both the real part and the imaginary part of $1/\tau_e(\omega)$ by using the memory-function approach which should be valid at arbitrary temperature. One effect of the imaginary part of $1/\tau_e(\omega)$ as can be seen from Eqs. (1) and (2) is to renormalize the resonance masses m_1 and m_2 .

The other effect of $\text{Im}[1/\tau_e(\omega)]$ is to correlate the cyclotron motions of these two types of carriers. However, it is more difficult to compare our work with Ref. 7. The authors there used the Fermi-liquid theory to evaluate the magnetoconductivity. However, the comparison is still possible if we expand the conductivity $\sigma_+(\omega)$ of Ref. 7 to the lowest order in the Fermi-liquid interacting parameter A_{12} , and identify it with the corresponding term in the conductivity defined in Eq. (4). A relation between A_{12} and $\tau_e^{-1}(\omega)$ can thus be obtained and it should depend on the magnetic field H and the single-particle scattering time τ_j . Since both A_{12} and

$\tau_e^{-1}(\omega)$ are calculated for zero magnetic field and τ_j ($j = 1, 2$) $\rightarrow \infty$, we have

$$A_{12} = \frac{i}{2\omega} \left[\frac{n_1 n_2}{m_1 m_2} \right]^{1/2} \frac{(m_2 - m_1)^2}{m_1 n_1 + m_2 n_2} \tau_e^{-1}(\omega). \quad (26)$$

The right-hand side of the above equation depends on ω and $\tau_e^{-1}(\omega)$ having both a real and an imaginary part. The value of A_{12} in Ref. 7 is evaluated at $T = 0$ and $\omega = 0$. It is real and independent of ω . Therefore, the above equation is valid only when $\omega \rightarrow 0$, where $\text{Re}[1/\tau_e(\omega)] \simeq \omega^2$ and $\text{Im}[1/\tau_e(\omega)] \simeq \omega$. From Eq. (26), it is straightforward to show that A_{12} corresponds to $\text{Im}1/\tau_e(\omega)$ in the $\omega \rightarrow 0$ and $T = 0$ limit. The finite temperature has also been studied by Takada⁷ where the value of A_{12} obtained at $\omega = 0$ and $T = 0$ has been used. We do not believe that such an approximation is reasonable because the value of A_{12} should change significantly when ω ($\simeq 3.5$ meV) or T is comparable to the Fermi energies $E_F^{(i)}$ ($i = 1, 2$).

Although our theory is able to explain some of the features in the experimental measurements, it is far from complete. For example, at high temperature, the phonon-mediated intervalley electron-electron scattering may become important. This scattering process would add to the intervalley electron-electron interaction and enhances the value of $\tau_e^{-1}(\omega)$. Thus the width of the cyclotron-resonance line shape may become larger and the cyclotron-resonance mass or masses may have additional temperature dependence. This effect has not been considered here, but will be subjected to a future study.

ACKNOWLEDGMENTS

One of us (C.S.T.) would like to thank Professor J. J. Quinn for helpful discussions. This work is supported in part by the Office of Naval Research and by the Army Research Office with Contract No. DAAG 29-09-C0039.

¹F. Stern and W. E. Howard, Phys. Rev. **163**, 861 (1967).

²G. Dorda, J. Eisele, and H. Gesch, Phys. Rev. B **17**, 1785 (1978).

³H. Kuhlbeck and J. P. Kotthaus, Phys. Rev. Lett. **35**, 1019 (1975).

⁴P. Stallhofer, J. P. Kotthaus, and J. F. Koch, Solid State Commun. **20**, 519 (1976).

⁵M. J. Kelley and L. M. Falicov, Phys. Rev. Lett. **37**, 1021 (1976); Phys. Rev. B **15**, 1983 (1977).

⁶J. Appel and A. W. Overhauser, Phys. Rev. B **18**, 758 (1978).

⁷Y. Takada and T. Ando, Phys. Soc. Jpn. **44**, 905 (1978); Y. Takada, Surf. Sci. **98**, 437 (1980).

⁸G. Abstreiter, P. Stallhofer, and J. P. Kotthaus, Surf. Sci. **98**, 413 (1980).

⁹A. K. Ganguly and C. S. Ting, Phys. Rev. B **16**, 3541 (1976).

¹⁰L. A. Kukkonen and P. E. Maldagne, Phys. Rev. Lett. **37**, 782 (1976).

¹¹W. Gotze and P. Wolfle, Phys. Rev. B **6**, 1226 (1972).

¹²J. J. Quinn (private communication).

¹³W. Lai, L. Y. Liou, and C. S. Ting (unpublished).

¹⁴C. S. Ting, Surf. Sci. **98**, 437 (1980).

¹⁵C. S. Ting, S. C. Ying, and J. J. Quinn, Phys. Rev. B **16**, 5394 (1977).

¹⁶A. A. Abrikosov, L. P. Gorkov, and I. E. Pzyaloshinski, in *Methods of Quantum Field Theory in Statistical Physics*, translated and edited by R. Silverman (Prentice-Hall, Englewood Cliffs, New Jersey, 1963).

¹⁷B. Vinter, Phys. Rev. Lett. **35**, 1044 (1975).

¹⁸W. Y. Lai and C. S. Ting (unpublished).